Speed Sensorless Predictive Current Control of a Five-Phase Induction Machine

Osvaldo Gonzalez*, Jorge Rodas*, Raul Gregor*, Magno Ayala* and Marco Rivera†

*Laboratory of Power and Control Systems, Facultad de Ingeniería, Universidad Nacional de Asunción

E-mail: {ogonzalez, jrodas, rgregor & mayala}@ing.una.py

†Department of Electrical Engineering, Universidad de Talca, Chile

E-mail: marcoriv@utalca.cl

***Abstract*—In power electronics, multiphase machines have been recently proposed, where most sensorless algorithms applied to electrical drives are represented through a mathematical representation of the physical system which includes the electrical and mechanical parameters of the motor. However, in electrical drive applications, the rotor current cannot be measured, so it must be estimated. This paper deals with the speed sensorless control of five-phase induction machines by using an inner loop of model-based predictive control (MPC). The MPC is obtained from the mathematical model of the machine, using a state-space representation where the two state variables are the stator and rotor currents, respectively. The rotor current is estimated using a reduced order optimal estimator based on a Kalman filter. Simulation results are provided to show the efficiency of the proposed sensorless speed control algorithm.**

***Index Terms*—Multiphase induction machine, five-phase induction machine, Kalman filter, sensorless control.**

I. Introduction

Multiphase machines have received considerable attention during the last few decades proposed for applications where some advantages such as improved reliability, fault tolerance, reduce torque pulsations and greater efficiency can be found in [1]. The five-phase induction machine (IM) is considered as the smallest phase number available in multiphase systems. High performance applications in multiphase machine require specific control systems, some methods used for controlling the five-phase IM including direct torque control [2], field oriented control [3] and model predictive control (MPC) [4].

This paper considers the speed control of symmetrical five-phase machines by using an inner loop of predictive current control based on the model, to predict the effects of future control actions on the state variables. In order to achieve this goal, the proposed algorithm uses reduced order estimators based on a Kalman filter (KF) to estimate the rotor current. Thereafter the rotor current estimate is used to determine an estimate of the speed of the machine. The performance of the proposed control technique in a symmetrical five-phase machine drive is studied for varying load and speeds operations.

The paper is organized as follows. Section II describes the five-phase induction machine model. Section III presents the mathematical model of the machine. Section IV details the predictive model with the speed observer and the current control with rotor current estimator based on KF. Section V presents the proposed predictive control method for the five-phase IM. Simulation results are provided in Section VI, showing the control performance with the rotor current estimation. Finally, concluding remarks are summarized in Section VII.

II. The Five-phase induction machine

The system studied consists of a symmetrical five-phase machine with distributed and equally displaced ($\vartheta = 2\pi/5$) windings fed by a five-phase two level VSI and a DC link. A detailed scheme of the drive is represented in Fig. 1.

This five-phase machine is a continuous system which can be described by a set of differential equations. The model of the system can be simplified by means of the vector space decomposition (VSD) introduced in [5]. By applying this technique, the original five-dimensional space of the machine is transformed into two-dimensional orthogonal subspaces in the stationary reference frame $(\alpha - \beta)$, $(x - y)$ and (z). This transformation is obtained by means of 5 x 5 transformation matrix:

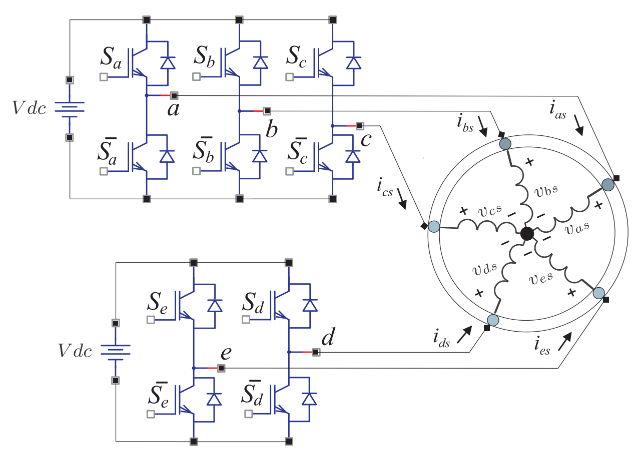

Fig. 1. Schematic diagram of the five-phase induction motor drive.

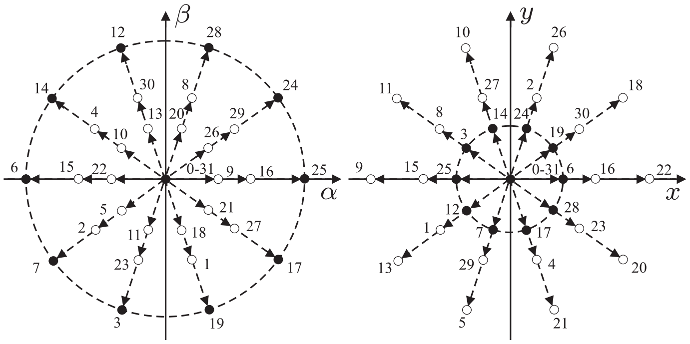

Fig. 2. Voltage space vectors and switching states in the $(\alpha-\beta)$ and $(x-y)$ subspaces for a five-phase symmetrical VSI.

$$\mathbf{T}=\frac{2}{5}\begin{bmatrix} 1 & \cos(\vartheta) & \cos(2\vartheta) & \cos(3\vartheta) & \cos(4\vartheta) \\ 0 & \sin(\vartheta) & \sin(2\vartheta) & \sin(3\vartheta) & \sin(4\vartheta) \\ 1 & \cos(2\vartheta) & \cos(4\vartheta) & \cos(\vartheta) & \cos(3\vartheta) \\ 0 & \sin(2\vartheta) & \sin(4\vartheta) & \sin(\vartheta) & \sin(3\vartheta) \\ \frac{1}{2} & \frac{1}{2} & \frac{1}{2} & \frac{1}{2} & \frac{1}{2} \end{bmatrix} \quad (1)$$

where an amplitude invariant criterion was used.

The VSI has a discrete nature, actually, it has a total number of $2^5 = 32$ different switching states defined by five switching functions corresponding to the five inverter legs $[S_a, ..., S_e]$ and their complementary values $[\overline{S}_a, ..., \overline{S}_e]$, where $\mathbf{S}_i \in \{0, 1\}$. The different switching states and the voltage of the DC link (Vdc) define the phase voltages which can in turn be mapped to the $(\alpha-\beta)-(x-y)$ space according to the VSD approach. For this reason, the 32 different on/off combinations of the five VSI legs lead to 32 space vectors in the $(\alpha-\beta)$ and $(x-y)$ subspaces. Fig. 2 shows the active vectors in the $(\alpha-\beta)$ and $(x-y)$ subspaces.

On the other hand, a transformation matrix must be used to represent the stationary reference frame $(\alpha-\beta)$ in the dynamic reference $(d-q)$. This matrix is given by:

$$\mathbf{T}_{dq}=\begin{bmatrix} cos\left(\delta_r\right) & -sin\left(\delta_r\right) \\ sin\left(\delta_r\right) & cos\left(\delta_r\right) \end{bmatrix} \quad (2)$$

where δ_r is the rotor angular position referred to the stator.

III. Machine Model

It is possible to model the machine by using an state-space representation, based on the VSD approach and the dynamic reference transformation. This model is given by:

$$\begin{aligned} \frac{d}{dt}\mathbf{X}_{\alpha\beta xy} &= \mathbf{A}\mathbf{X}_{\alpha\beta xy}+\mathbf{B}\mathbf{U}_{\alpha\beta xy} \\ \mathbf{Y}_{\alpha\beta xy} &= \mathbf{C}\mathbf{X}_{\alpha\beta\mathbf{xy}} \end{aligned} \quad (3)$$

where $\mathbf{U}_{\alpha\beta xy} = \left[\; u_{\alpha s}\, u_{\beta s}\, u_{xs}\, u_{ys}\, 0\, 0 \;\right]^T$ represents the input vector, $\mathbf{X}_{\alpha\beta xy} = \left[\; i_{\alpha s}\, i_{\beta s}\, i_{xs}\, i_{ys}\, i_{\alpha r}\, i_{\beta r} \;\right]^T$ denotes the state vector, $\mathbf{Y}_{\alpha\beta xy} = \left[\; i_{\alpha s}\, i_{\beta s}\, i_{xs}\, i_{ys}\, 0\, 0 \;\right]^T$ indicates the output vector and $\mathbf{A}$, $\mathbf{B}$ and $\mathbf{C}$ are matrices that define the dynamics of the electrical drive.

The mechanical part of the electrical drive is given by the following equations:

$$T_e = \frac{5}{2}P\left(\psi_{\alpha s}i_{\beta s} - \psi_{\beta s}i_{\alpha s}\right) \quad (4)$$

$$J_i\frac{d}{dt}\omega_r + B_i\omega_r = P\left(T_e - T_L\right) \quad (5)$$

where T_L denotes the load torque, T_e is the generated torque, J_i the inertia coefficient, P the number of pairs of poles, $\psi_{\alpha s}$ and $\psi_{\beta s}$ the stator flux and B_i the friction coefficient.

IV. Predictive Model

Assuming the mathematical model expressed by (3) and using the state variables defined by the vector $[\mathbf{x}]_{\alpha\beta xy}$, we can define the following set of equations:

$$\begin{aligned} \dot{x_1} &= c_3\left(R_r x_5 + \omega_r x_6 L_r + \omega_r x_2 L_m\right) \\ &\quad + c_2\left(u_{\alpha s} - R_s x_1\right) \\ \dot{x_2} &= c_3\left(R_r x_6 - \omega_r x_5 L_r - \omega_r x_1 L_m\right) \\ &\quad + c_2\left(u_{\beta s} - R_s x_2\right) \\ \dot{x_3} &= -R_s c_4 x_3 + c_4 u_{xs} \\ \dot{x_4} &= -R_s c_4 x_4 + c_4 u_{ys} \\ \dot{x_5} &= -R_s c_3 x_1 + c_5\left(-L_m\omega_r x_2 - R_r x_5 - L_r\omega_r x_6\right) \\ &\quad - c_3 u_{\alpha s} \\ \dot{x_6} &= -R_s c_3 x_2 + c_5\left(L_m\omega_r x_1 + L_r\omega_r x_5 - R_r x_6\right) \\ &\quad - c_3 u_{\beta s} \end{aligned} \quad (6)$$

where c_i $(i = 1, ..., 5)$ are constants defined as:

$$c_1 = L_s L_r - L_m^2,\; c_2 = \frac{L_r}{c_1},\; c_3 = \frac{L_m}{c_1},\; c_4 = \frac{1}{L_{ls}},\; c_5 = \frac{L_s}{c_1} \quad (7)$$

and ω_r is the rotor angular speed, R_s, $L_s = L_{ls} + L_m$, R_r, $L_r = L_{lr} + L_m$ and L_m are the electrical parameters of the machine.

Stator voltages are related to the input control signals through the inverter model. In this case, the simplest model has been considered for the sake of speeding up the optimization process. Then if the gating signals are arranged in the vector $\mathbf{S} = [S_a,\, S_b,\, S_c,\, S_d,\, S_e,] \in \mathbf{R}^5$, where $\mathbf{R} = \{0, 1\}$ the stator voltages can be obtained from:

$$\mathbf{M}=\frac{1}{5}\begin{bmatrix} 4 & -1 & -1 & -1 & -1 \\ -1 & 4 & -1 & -1 & -1 \\ -1 & -1 & 4 & -1 & -1 \\ -1 & -1 & -1 & 4 & -1 \\ -1 & -1 & -1 & -1 & 4 \end{bmatrix}\begin{bmatrix} S_a \\ S_b \\ S_c \\ S_d \\ S_e \end{bmatrix} \quad (8)$$

An ideal inverter converts gating signals into stator voltages that can be projected to $(\alpha-\beta)$ and $(x-y)$ subspaces and gathered in a row vector $\mathbf{U}_{\alpha\beta xys}$ computed as:

$$\mathbf{U}_{\alpha\beta xys} = [u_{\alpha s},\, u_{\beta s},\, u_{xs},\, u_{ys},\, 0,\, 0]^T = Vdc \cdot \mathbf{T} \cdot \mathbf{M} \quad (9)$$

being Vdc the DC link voltage and the superscript (^{T}) indicates the transposed matrix. Applying the rotational transformation (2) to the $(\alpha - \beta)$ components, we can obtain:

$$\mathbf{U}_{dqs} = [u_{ds},\, u_{qs}]^T = \mathbf{T}_{dq} \cdot \begin{bmatrix} u_{\alpha s} \\ u_{\beta s} \end{bmatrix} \tag{10}$$

By combining the equations (6)-(10) a nonlinear set of equations arises that can be written in state space form:

$$\begin{aligned} \dot{\mathbf{X}}(t) &= f\,[\mathbf{X}(t),\, \mathbf{U}(t)] \\ \mathbf{Y}(t) &= \mathbf{C}\mathbf{X}(t) \end{aligned} \tag{11}$$

with state vector $\mathbf{X}(t) = [x_1,\, x_2,\, x_3,\, x_4,\, x_5,\, x_6]^T$, input vector $\mathbf{U}(t) = [u_{\alpha s},\, u_{\beta s},\, u_{xs},\, u_{ys}]$, and output vector $\mathbf{Y}(t) = [i_{\alpha s},\, i_{\beta s},\, i_{xs},\, i_{ys}]^T$. The components of the vectorial function f and the matrix $\mathbf{C}$ are obtained in a straightforward manner from (6) and the definitions of state and output vector. Model (11) must be discretized in order to be of used for the predictive controller. A forward Euler method is used to keep a low computational cost. Due to this fact, the resulting equations will have the required digital control form, with predicted variables depending just on past values and not on present values of the variables. Thus, a prediction of the future next-sample state $\hat{\mathbf{X}}_{[k+1|k]}$ is expressed as:

$$\hat{\mathbf{X}}_{[k+1|k]} = f\left(\mathbf{X}_{[k]},\, \mathbf{U}_{[k]},\, T_m,\, \omega_{r[k]}\right) \tag{12}$$

where k is the current sample and T_m the sampling time.

A. Reduced order estimators

In the state space description (11) only stator currents, voltages and mechanical speed are measured. Stator voltages are easily predicted from the gating commands issued to the VSI, rotor current, however, cannot be directly measured. This difficulty can be overcome by means of estimating the rotor current using the concept of reduced order estimators.

The reduced order estimators provide an estimate for only the unmeasured part of the state vector, then, the evolution of states can be written as:

$$\underbrace{\begin{bmatrix} \hat{\mathbf{X}}_{a[k+1|k]} \\ \hat{\mathbf{X}}_{b[k+1|k]} \\ \hat{\mathbf{X}}_{c[k+1|k]} \end{bmatrix}}_{[\hat{\mathbf{X}}_{[k+1|k]}]} = \underbrace{\begin{bmatrix} \overline{\mathbf{A}}_{11} & \overline{\mathbf{A}}_{12} & \overline{\mathbf{A}}_{13} \\ \overline{\mathbf{A}}_{21} & \overline{\mathbf{A}}_{22} & \overline{\mathbf{A}}_{23} \\ \overline{\mathbf{A}}_{31} & \overline{\mathbf{A}}_{32} & \overline{\mathbf{A}}_{33} \end{bmatrix}}_{[\mathbf{A}]} \underbrace{\begin{bmatrix} \mathbf{X}_{a[k]} \\ \mathbf{X}_{b[k]} \\ \mathbf{X}_{c[k]} \end{bmatrix}}_{[\mathbf{X}_{[k]}]} + \underbrace{\begin{bmatrix} \overline{\mathbf{B}}_1 \\ \overline{\mathbf{B}}_2 \\ \overline{\mathbf{B}}_3 \end{bmatrix}^T}_{[\mathbf{B}]} \underbrace{\begin{bmatrix} \mathbf{U}_{\alpha\beta s} \\ \mathbf{U}_{xys} \\ \mathbf{U}_{\alpha\beta s} \end{bmatrix}}_{[\mathbf{U}_k]} \tag{13}$$

$$\mathbf{Y}_{[k]} = \underbrace{\begin{bmatrix} \overline{\mathbf{I}} & \overline{\mathbf{I}} & \overline{\mathbf{0}} \end{bmatrix}}_{[\mathbf{C}]} \underbrace{\begin{bmatrix} \mathbf{X}_{a[k]} \\ \mathbf{X}_{b[k]} \\ \mathbf{X}_{c[k]} \end{bmatrix}}_{[\mathbf{X}_{[k]}]} \tag{14}$$

where $\mathbf{X}_a = [i_{\alpha s} i_{\beta s}]^T$, $\mathbf{X}_b = [i_{xs} i_{ys}]^T$, $\mathbf{X}_c = [i_{\alpha r} i_{\beta r}]^T$, $\mathbf{U}_{\alpha\beta s} = [U_{\alpha s} U_{\beta s}]^T$, $\mathbf{U}_{xys} = [U_{xs} U_{ys}]^T$, [A] and [B] are matrices that depend on the electrical parameters of the machine and the sampling time T_m. Matrix [A] also depends on the actual value of $\omega_{r[k]}$, and it must be calculated every sampling time [6].

B. Rotor state estimation based on Kalman filters

The KF design considers uncorrelated process and zero-mean Gaussian measurement noises, thus the systems equations can be written as:

$$\hat{\mathbf{X}}_{[k+1]} = \mathbf{A}\mathbf{X}_{[k]} + \mathbf{B}\mathbf{U}_{[k]} + \mathbf{H}\varpi_{[k]} \tag{15}$$

$$\mathbf{Y}_{[k+1]} = \mathbf{C}\mathbf{X}_{[k+1]} + \nu_{[k+1]} \tag{16}$$

where $\varpi_{[k]}$ is the process noise, H is the noise weight matrix and $\nu_{[k+1]}$ is the measurement noise.

The dynamics of the KF are can be written as follows:

$$\begin{aligned} \hat{\mathbf{X}}_{c[k+1|k]} = (\mathbf{A}_{33} - \mathbf{K}_{[k]}\mathbf{A}_{13})\hat{\mathbf{X}}_{c[k]} + \mathbf{K}_{[k]}\mathbf{Y}_{[k+1]} + \\ (\mathbf{A}_{31} - \mathbf{K}_{[k]}\mathbf{A}_{11})\mathbf{Y}_{[k]} + (\mathbf{B}_3 - \mathbf{K}_{[k]}\mathbf{B}_1)\mathbf{U}_{\alpha\beta s[k]} \end{aligned} \tag{17}$$

being $\mathbf{K}_{[k]}$ the KF gain matrix that is calculated from the covariance of the noises at each sampling time in a recursive manner as:

$$\mathbf{K}_{[k]} = \mathbf{\Gamma}_{[k]} \cdot \mathbf{C}^T \widehat{R}_\nu^{-1} \tag{18}$$

being $\mathbf{\Gamma}_{[k]}$ the covariance of the new estimation, which it is defined like a function of the old covariance estimation (φ) as follows:

$$\mathbf{\Gamma}_{[k]} = \varphi_{[k]} - \varphi_{[k]} \cdot \mathbf{C}^T(\mathbf{C} \cdot \varphi_{[k]} \cdot \mathbf{C}^T + \widehat{R}_\nu)^{-1} \cdot \mathbf{C} \cdot \varphi_{[k]} \tag{19}$$

From the state equation, which includes the process noise, it is possible to obtain a correction of the covariance of the estimated state as:

$$\varphi_{[k+1]} = \mathbf{A}\mathbf{\Gamma}_{[k]} \cdot \mathbf{A}^T + \mathbf{H}\widehat{Q}_\varpi \cdot \mathbf{H}^T \tag{20}$$

This completes the required relations for the optimal state estimation using KF with PCC. Thus, $\mathbf{K}_{[k]}$ provides the minimum estimation errors, given a knowledge of the process noise magnitude ($\widehat{Q}_\varpi$), the measurement noise magnitude ($\widehat{R}_\nu$), and the covariance initial condition ($\varphi_{[0]}$).

This optimal design of the KF by means of a robust covariance estimation neither is a common subject in the field or is the purpose of our work, which is mainly focused in a proof of concept study of the predictive-fixed switching frequency technique. In our case, the KF gains will be tuned based on a heuristic method. Then, it is assumed that the estimated rotor state will produce sub-optimal results, which can be improved using more appropriate KF design methods.

C. Speed observer

After calculating the unmeasurable state variables, the speed can be estimated from the dynamic equation that models the mechanical part of the electrical drive (4) and (5) using the Euler discretization method. Thus the discrete equation which estimates the speed can be written as:

$$\hat{\omega}_{r[k+1]} = (1 - \frac{T_m B_i}{J_i})\hat{\omega}_{r[k]} + \frac{T_m P}{J_i}(T_{e[k]} - T_{L[k]}) \tag{21}$$

where it is assumed $\omega_{r[0]} = 0$, $T_{L[0]} = 0$ and the unmeasured states $i_{\alpha\beta r[0]} = 0$.

D. Torque observer

The load torque measurement is almost inapplicable, so it must be observed. Therefore, it's used the observer based on Gopinanth's method in its discrete version [7].

$$\begin{bmatrix}\epsilon_{1[k+1]}\\ \epsilon_{2[k+1]}\end{bmatrix} = \begin{bmatrix}1 & -k_1T_m\\ T_m & (1-k_2T_m)\end{bmatrix}\begin{bmatrix}\epsilon_{1[k]}\\ \epsilon_{2[k]}\end{bmatrix} + T_m\begin{bmatrix}k_1bJ_i\\ (k_2^2-k_1)J_i\end{bmatrix}\hat{\omega}_{r[k]} + T_m\begin{bmatrix}k_1\\ k_2\end{bmatrix}T_{e[k]} \tag{22}$$

$$\hat{T}_{L[k+1]} = \epsilon_{2[k+1]} - k_2J_i\hat{\omega}_{r[k+1]} \tag{23}$$

where k_1, k_2 and b are observer coefficients, ϵ_1 and ϵ_2 are internal state variables, T_e is the calculated motor electromagnetic torque and $\hat{T}_L$ is the calculated motor load torque.

E. Cost function

The cost function should include all terms to be optimized. In current control the most important figure is the tracking error in the predicted stator currents for the next sample. To minimize its magnitude for each sample k it suffices to use a simple expression such as:

$$\begin{aligned}J_{[k+2|k]} &= \hat{e}_{i\alpha s[k+2]} + \hat{e}_{i\beta s[k+2]} + \lambda_{xy}\left(\hat{e}_{ixs[k+2]} + \hat{e}_{iys[k+2]}\right)\\ \hat{e}_{i\alpha s[k+2]} &= \parallel i^*_{\alpha s[k+2]} - \hat{i}_{\alpha s[k+2]} \parallel^2\\ \hat{e}_{i\beta s[k+2]} &= \parallel i^*_{\beta s[k+2]} - \hat{i}_{\beta s[k+2]} \parallel^2\\ \hat{e}_{ixs[k+2]} &= \parallel i^*_{xs[k+2]} - \hat{i}_{xs[k+2]} \parallel^2\\ \hat{e}_{iys[k+2]} &= \parallel i^*_{ys[k+2]} - \hat{i}_{ys[k+2]} \parallel^2\end{aligned} \tag{24}$$

where $\parallel . \parallel$ denotes vector magnitude, $i^*_{s[k+2]}$ is a vector containing the reference for the stator currents and $\hat{i}_{s[k+2]}$ is a vector containing the predictions based on the next state and the control effort. More complicated cost functions can be devised for instance to minimize the harmonic content and/or the VSI losses [5],[8],[9].

F. Optimizer

The predictive model should be evaluate 32 (2^5) times in order to consider all possible voltage vectors. Fig. 2 shows the redundancy of the switching state results. This consideration is commonly known as the optimal solution. To make things clearer, a flow chart of the proposed control algorithm is provided in Fig. 4.

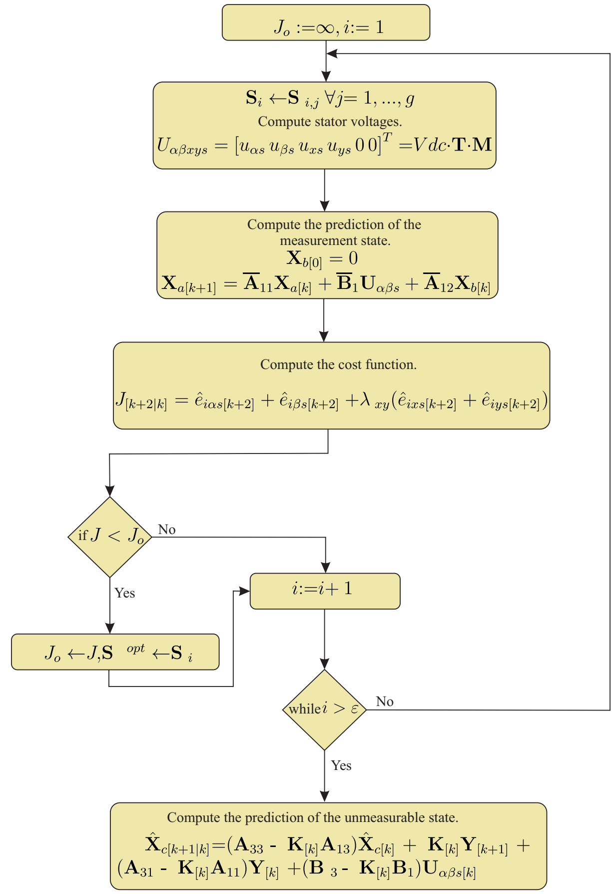

Fig. 4. Optimization algorithm.

V. Proposed predictive control method

From the point of view of the inner loop of the current control, conventional predictive control avoids the use of proportional-integer (PI) controllers and modulation techniques since a single switching vector is applied during the whole switching period. This procedure is somewhat similar to original DTC schemes and leads to variable switching frequency. The proposed control technique selects the control actions by solving an optimization problem for each sampling period. A model of the real system, which is the symmetrical five-phase induction machine, is used to predict its output. This prediction is carried out for each possible output, or switching vector, of the five-phase inverter to determine which one minimizes a defined cost function, and therefore, the model of the real system, also called predictive model, must be used considering all possible voltage vectors in the five-phase inverter. As the rotor current can not be measured directly, it should be estimated using a reduced order estimator based on KF. Different cost functions can be used, to express different control criteria. The absolute current error, in stationary reference frame $(\alpha - \beta)$ for the next sampling instant is normally used for computational simplicity. In this case, the cost function is defined as (24), where $i^*_{\alpha\beta[k+1]}$ is the stator reference current and $i_{\alpha\beta[k+2]}$ is the predicted stator current which is computationally obtained using the predictive model.

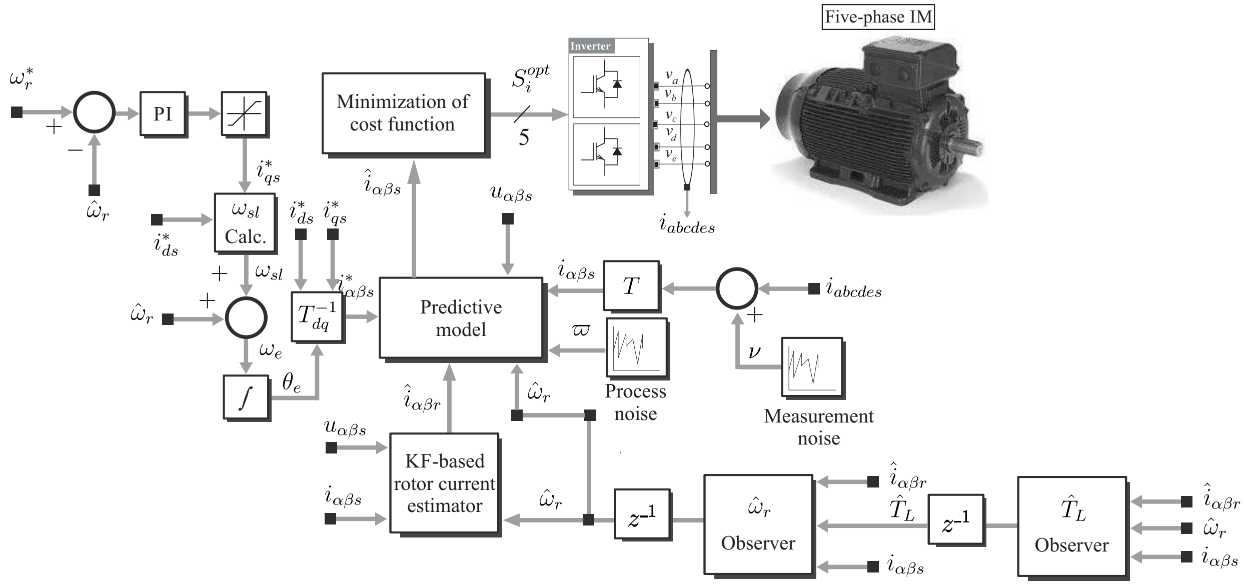

Fig. 3. Speed sensorles control with an inner current control based on MPC method and using KF for rotor current estimation.

However, other cost functions can be established, including harmonics minimization, switching stress or VSI losses [10]. Proportional integral (PI) controller with saturator is used in the speed sensorless control loop, based on the indirect vector control schema because of its simplicity. In the indirect vector control scheme, PI speed controller is used to generate the reference current i^*_{ds} in dynamic reference frame. The current reference used by the predictive model are obtained from the calculation of the electric angle used to convert the current reference, originally in dynamic reference frame $(d-q)$, to static reference frame $(\alpha-\beta)$. The process of calculation of the slip frequency (ω_{sl}) is performed in the same manner as the Indirect Field Orientation methods, from the reference currents in dynamic reference frame (i^*_{ds}, i^*_{qs}) and the electrical parameters of the machine (R_r, L_r). Finally, using the rotor current estimated, the stator current measured and the load torque measured from the induction machine we can estimate the speed of the machine. A detailed block diagram of the proposed sensorless speed control technique for the symmetrical five-phase induction motor drive is provided in Fig. 3.

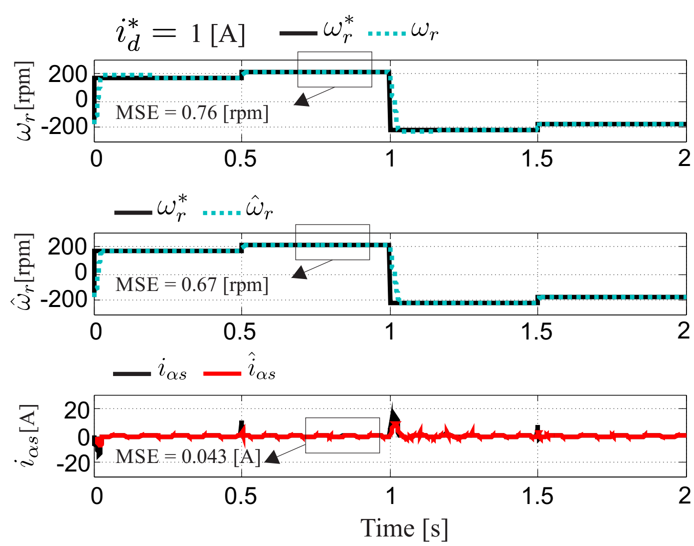

Fig. 5. Simulation results for a multi-step speed references application.

VI. Simulation Results

A MATLAB/Simulink simulation environment has been designed for the VSI-fed five-phase IM, and simulations have been performed to show the efficiency of the proposed predictive speed control technique. Numerical integration using first order Euler's method algorithm has been applied to compute the evolution of the state variables step by step in the time domain.

The efficiency of the proposed speed sensorless control algorithm for the symmetrical five-phase induction machine has been evaluated, under load conditions. In all cases is considered a sampling frequency of 10 kHz. Fig. 5 shows the simulation results for a multi-step speed references [180, 220, -220, -180] revolutions per minute (rpm), if we consider a fixed reference current (i^*_{ds} = 1 A). The subscripts $(\alpha-\beta)$ represent quantities in the stationary frame reference of the stator currents. The estimated speed is fedback into the closed loop for speed regulation and a PI controller is used in the speed regulation loop as shown in Fig. 3. Furthermore, it can be seen from this graph, the change in the phases of the stator currents in the $(\alpha-\beta)$ subspace, caused by the reversal of the direction of rotation of the machine. Under these test conditions, the mean squared error (MSE) in the speed and current tracking (in steady state) are 0.76 rpm, 0.67 rpm and 0.043 A, respectively.

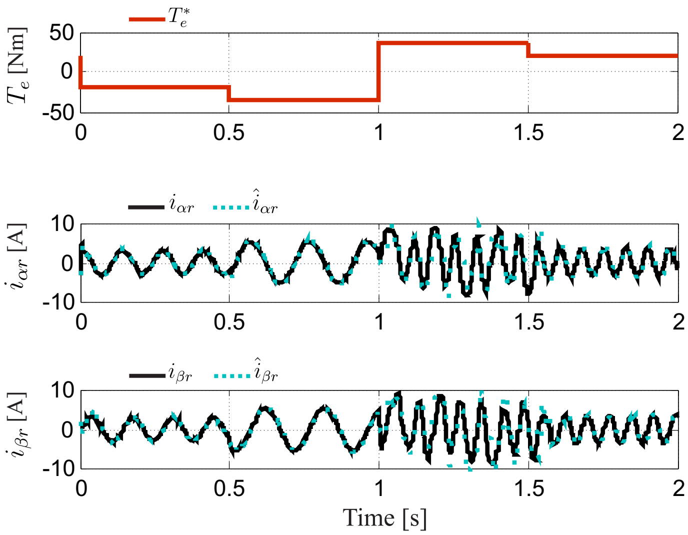

Fig. 6. Simulation results for a multi-step load torque application.

Fig. 6 shows a multi-step load torque application response [-20, -35, 35, 20] N·m, and the rotor current evolution (measured and observed) in a stationary reference frame. It can be seen in this graph the amplitude variation of the rotor current in function to the load torque applied to the machine. These simulation results substantiate the expected performance of the proposed algorithm, based on a reduced order estimator which uses a KF. The estimated rotor current converges to real values for these test conditions as shown in figures, proving that the observed performance is satisfactory.

VII. Conclusion

This paper proposes a sensorless speed control scheme using an inner loop based on the predictive current control in five-phase induction machine. The model-based predictive control is described using a state-space representation, where the rotor and stator current are the state variables. As the rotor current cannot be measured, it is estimated using an optimal estimator based on a Kalman filter. The theoretical development of the estimator has been validated by simulation results. The method avoids the use of modulation techniques and has proven to be efficient even when considering that the machine is operating under varying load and speeds regimes.

Appendix

Electrical and mechanical parameters for the five-phase IM:

$R_s = 12.8\Omega$, $R_r = 4.79\Omega$, $L_s = 757.92$mH, $L_r = 757.92$mH, $L_m = 272$ mH, $J_i = 0.02$ kg·m^2, $B_i = 35.983 \times 10^{-3}$ kg·m^2/s, $f_a = 50$ Hz, $p = 3$.

Acknowledgment

The authors would like to thank to the Paraguayan Government for the economical support provided by means of a CONACYT grant project 14-INV-101.

References

[1] M. J. Duran and F. Barrero, "Recent advances in the design, modeling, and control of multiphase machines part i," *Industrial Electronics, IEEE Transactions on*, vol. 63, no. 1, pp. 459–468, 2016.

[2] L. Zheng, J. E. Fletcher, B. W. Williams, and X. He, "A novel direct torque control scheme for a sensorless five-phase induction motor drive," *Industrial Electronics, IEEE Transactions on*, vol. 58, no. 2, pp. 503–513, 2011.

[3] H. Guzman, M. J. Duran, F. Barrero, B. Bogado, and S. Toral, "Speed control of five-phase induction motors with integrated open-phase fault operation using model-based predictive current control techniques," *Industrial Electronics, IEEE Transactions on*, vol. 61, no. 9, pp. 4474–4484, 2014.

[4] S. Bayhan, H. Abu-Rub, and O. Ellabban, "Sensorless model predictive control scheme of wind-driven doubly fed induction generator in dc microgrid," *IET Renewable Power Generation*, vol. 10, no. 4, pp. 514–521, 2016.

[5] Y. Zhao and T. A. Lipo, "Space vector pwm control of dual three-phase induction machine using vector space decomposition," *Industry Applications, IEEE Transactions on*, vol. 31, no. 5, pp. 1100–1109, 1995.

[6] J. Rodas, H. Guzman, R. Gregor, and F. Barrero, "Model predictive current controller using kalman filter for fault-tolerant five-phase wind energy conversion systems," in *PEDG 2016-7th International Symposium on Power Electronics for Distributed Generation Systems*. IEEE, 2016.

[7] R. Gregor and J. Rodas, "Speed sensorless control of dual three-phase induction machine based on a luenberger observer for rotor current estimation," in *IECON 2012 - 38th Annual Conference on IEEE Industrial Electronics Society*, Oct 2012, pp. 3653–3658.

[8] R. Gregor, J. Rodas, J. Munoz, M. Ayala, O. Gonzalez, and D. Gregor, "Predictive-fixed switching frequency technique for 5-phase induction motor drives," in *SPEEDAM 2016-23th International Symposium on Power Electronics, Electrical Drives, Automation and Motion*. IEEE, 2016.

[9] S. Kwak and S.-k. Mun, "Model predictive control methods to reduce common-mode voltage for three-phase voltage source inverters," *IEEE Transactions on Industrial Electronics*, vol. 30, no. 9, pp. 5019–5035, 2015.

[10] V. Kumar, P. Gaur, and A. P. Mittal, "Finite-state model predictive control of npc inverter using multi-criteria fuzzy decision-making," *International Transactions on Electrical Energy Systems*, vol. 25, no. 5, pp. 876–897, 2015.